

GL-TR-90-0106

**AD-A224 488**

**Frequency Dependence and Spatial Distribution  
of Seismic Attenuation in France: Experimental  
Results and Possible Interpretations**

M. Campillo  
J. L. Plantet

Radiomana - Societe Civile  
27 Rue Claude Bernard  
75005 Paris, FRANCE

12 September 1989

Scientific Report No. 2

**APPROVED FOR PUBLIC RELEASE; DISTRIBUTION UNLIMITED**

**DTIC**  
**ELECTE**  
JUL 31 1990  
**S** **D**  
a  
**E**

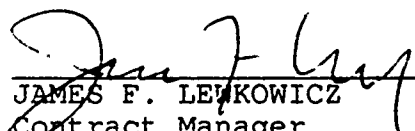
GEOPHYSICS LABORATORY  
AIR FORCE SYSTEMS COMMAND  
UNITED STATES AIR FORCE  
HANSCOM AIR FORCE BASE, MASSACHUSETTS 01731-5000

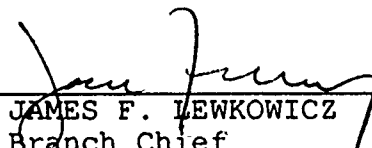
SPONSORED BY  
Defense Advanced Research Projects Agency  
Nuclear Monitoring Research Office  
ARPA ORDER NO 5299

MONITORED BY  
Geophysics Laboratory  
AFOSR-87-0331

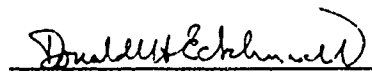
The views and conclusions contained in this document are those of the authors and should not be interpreted as representing the official policies, either expressed or implied, of the Defense Advanced Research Projects Agency or the U.S. Government.

This technical report has been reviewed and is approved for publication.

  
\_\_\_\_\_  
JAMES F. LEWKOWICZ  
Contract Manager  
Solid Earth Geophysics Branch  
Earth Sciences Division

  
\_\_\_\_\_  
JAMES F. LEWKOWICZ  
Branch Chief  
Solid Earth Geophysics Branch  
Earth Sciences Division

FOR THE COMMANDER

  
\_\_\_\_\_  
DONALD H. ECKHARDT, Director  
Earth Sciences Division

This report has been reviewed by the ESD Public Affairs Office (PA) and is releasable to the National Technical Information Service (NTIS).

Qualified requestors may obtain additional copies from the Defense Technical Information Center. All others should apply to the National Technical Information Service.

If your address has changed, or if you wish to be removed from the mailing list, or if the addressee is no longer employed by your organization, please notify GL/IMA, Hanscom AFB, MA 01731-5000. This will assist us in maintaining a current mailing list.

Do not return copies of this report unless contractual obligations or notices on a specific document requires that it be returned.

REPORT DOCUMENTATION PAGE				Form Approved OMB No. 0704-0188	
1a. REPORT SECURITY CLASSIFICATION Unclassified		1b. RESTRICTIVE MARKINGS			
2a. SECURITY CLASSIFICATION AUTHORITY		3. DISTRIBUTION/AVAILABILITY OF REPORT Approved for public release			
2b. DECLASSIFICATION/DOWNGRADING SCHEDULE		Distribution unlimited			
4. PERFORMING ORGANIZATION REPORT NUMBER(S)		5. MONITORING ORGANIZATION REPORT NUMBER(S) GL-TR-90-0106			
6a. NAME OF PERFORMING ORGANIZATION Radiomana - Société Civile		6b. OFFICE SYMBOL (If applicable)	7a. NAME OF MONITORING ORGANIZATION European Office of Aerospace and Development		
6c. ADDRESS (City, State, and ZIP Code) 27 rue Claude Bernard 75005 Paris France		7b. ADDRESS (City, State, and ZIP Code) Box 14 FPO New York 09510 - 0200			
8a. NAME OF FUNDING/SPONSORING ORGANIZATION Geophysics Laboratory		8b. OFFICE SYMBOL (If applicable)	9. PROCUREMENT INSTRUMENT IDENTIFICATION NUMBER AFOSR - 87 - 0331 - A		
8c. ADDRESS (City, State, and ZIP Code) Hanscom AFB MA 01731 - 5000		10. SOURCE OF FUNDING NUMBERS			
		PROGRAM ELEMENT NO. 61101 E	PROJECT NO. 7 A 10	TASK NO. D A	WORK UNIT ACCESSION NO. C Z
11. TITLE (Include Security Classification) Frequency dependence and spatial distribution of seismic attenuation in France : experimental results and possible interpretations.					
12. PERSONAL AUTHOR(S) M. Campillo and J.L. Plantet					
13a. TYPE OF REPORT Scientific Report #2		13b. TIME COVERED FROM 7/15/88 TO 7/14/89		14. DATE OF REPORT (Year, Month, Day) 1989 September 12	15. PAGE COUNT 56
16. SUPPLEMENTARY NOTATION					
17. COSATI CODES			18. SUBJECT TERMS (Continue on reverse if necessary and identify by block number)		
FIELD	GROUP	SUB-GROUP	Seismic waves - Regional phases - Lg, Pg phases - Attenuation - Q factor - Scattering - Crust -		
19. ABSTRACT (Continue on reverse if necessary and identify by block number)					
<p>→ We processed digital records from 431 earthquakes at 25 stations of LDG network in France. We computed spectral amplitudes of Pg and Lg in different group velocity windows. We used this large data set to compute a map of mean crustal attenuation by evaluating simultaneously source amplitude, site response and apparent Q. We used a procedure combining an iterative reconstruction technique with an adjustment of source amplitudes and site responses at each step of the inversion. The stability of the results is tested with different subsets of data and the resolution is evaluated. We obtained maps of apparent attenuation at frequencies between 1.5 and 10 Hz, computed from Pg, Lg and early coda of Lg. The results obtained are in a good agreement with the predictions of the single scattering model both for frequency dependence and Qs-Qp ratio. The comparison between the attenuation anomaly found in the Variscan belt and a deep reflexion seismic profile confirms the prominent part played by scattering for the apparent attenuation of seismic waves in the crust.</p>					
20. DISTRIBUTION/AVAILABILITY OF ABSTRACT <input checked="" type="checkbox"/> UNCLASSIFIED/UNLIMITED <input type="checkbox"/> SAME AS RPT <input type="checkbox"/> DTIC USERS			21. ABSTRACT SECURITY CLASSIFICATION Unclassified		
22a. NAME OF RESPONSIBLE INDIVIDUAL James Lewkowicz		22b. TELEPHONE (Include Area Code) ( 617 ) 377 - 3028		22c. OFFICE SYMBOL GL - LWH	

Unclassified  
 Keywords: seismic data/reflection; Earth crust, Regional phases; seismic attenuation/scattering. (EDC)4  
 A

## CONTENTS

Introduction	3
Data Processing	6
Data Analysis	7
Algorithm of Inversion	10
Accuracy of the Results	13
Results Obtained at 3 Hz	17
Frequency Dependence of $Q_s$ Inferred From $L_{g1}$	18
Frequency Dependence of $Q_p$ Inferred From $P_g$	20
Discussion of the Mean Values of Apparent $Q_s$	20
Discussion of the Spatial Distribution of Apparent Attenuation	22
Conclusion	24
References	25

## ILLUSTRATIONS

1. Locations of Earthquakes (squares) and Stations (black dots) Used in This Study	31
2. Path Coverage at a Frequency of 3 Hz	32
3. Scheme of Data Processing and Inversion	33
4. Results Obtained With Different Subsets of 25, 25, 55, and 100 Events	34
5. Resolution Maps Relative to 6 Different Locations	35
6. Results Obtained at 3 Hz for the 4 Group Velocity Windows Considered	36
7. Results Obtained for the Group Velocity Window $L_{g1}$ at Different Frequencies	37
8. Results Obtained for $Q_p$ in the Group Velocity Window Corresponding to $P_g$	38
9. Frequency Dependence of the Quality Factor for P and S Waves After Correction of Our Result From a Frequency Independent Intrinsic $Q$ of 1500	39

10. Wide Angle Reflection Profile Showing a Zone of Strong Heterogeneity in the Crust (after Matte and Hirn, 1988) and the Apparent Qs Inferred From Lg (Lg1)

40



Accession For	
NTIS GRA&I	<input checked="" type="checkbox"/>
DTIC TAB	<input type="checkbox"/>
Unannounced	<input type="checkbox"/>
Justification	
By _____	
Distribution/	
Availability Codes	
Dist	Avail and/or Special
A-1	

Frequency dependence and spatial distribution of  
seismic attenuation in France:  
experimental results and possible interpretations.

M. Campillo

Laboratoire de Geophysique Interne et Tectonophysique Universite  
Joseph Fourier and Observatoire de Grenoble IRIGM, BP 53X, 38041  
Grenoble, France

J.L. Plantet

Laboratoire de Detection Geophysique Commissariat a l'Energie  
Atomique BP 12, 91680 Bruyere-le-Chatel, France

**Abstract:**

We processed digital records from 431 earthquakes at 25 stations of LDG network in France. We computed spectral amplitudes of Pg and Lg in different group velocity windows. We used this large data set to compute a map of mean crustal attenuation by evaluating simultaneously source amplitude, site response and apparent Q. We used a procedure combining an iterative reconstruction technique with an adjustment of source amplitudes and site responses at each step of the inversion. The stability of the result is tested with different subsets of data and the resolution is evaluated. We obtained maps of apparent attenuation at frequencies between 1.5 and 10 Hz, computed from Pg, Lg and early coda of Lg.

The results obtained are in a good agreement with the predictions of the single scattering model both for frequency dependence and  $Q_s$ - $Q_p$  ratio. The comparison between the attenuation anomaly found in the Variscan belt and a deep reflexion seismic profile confirms the prominent part played by scattering for the apparent attenuation of seismic waves in the crust.

## Introduction

The short period seismic phases Pg and Lg have been extensively studied for the purposes of nuclear test monitoring, magnitude determination or attenuation measurements (e.g. Nuttli, 1973, 1986). Considering regions in which a flat layering can be regarded as a reasonable model for the earth crust, the mode of propagation of these phases has been clearly established by the comparison between observed and theoretical properties. The theoretical results were obtained considering oversimplified models of the crust which consist of stacks of a few flat visco-elastic layers, each of them being considered as homogeneous at any scale. Nevertheless, these numerical simulations fail to explain several very general features of regional phases. The long duration of the signals (the existence of a coda) in most of the observations is not accounted for. Similarly, to explain the actual attenuation of these signals, it is necessary to include in the models a frequency dependent quality factor that is not compatible with accepted processes of intrinsic attenuation at depth. These phenomena are generally attributed to the scattering due to unprecisely defined heterogeneities that have to be added to the vertical layering usually hypothesized. The description of crustal heterogeneity can be separated into two parts. The first one deals with the small scale heterogeneity that consists of the fluctuations of the elastic properties at a scale roughly

equal or smaller than the wavelengths considered in short period seismology. These fluctuations cannot be described in a deterministic point of view because the detail of the crustal structure is far beyond our present knowledge. The implications of this type of heterogeneity were studied in detail, particularly to explain the coda of local seismograms and the frequency dependence of the apparent attenuation. Since the pioneering work of Aki (1969), it has been now clearly established that scattering on small fluctuations of elastic parameters can account, at least partially, for the existence of coda and for the frequency dependence of apparent attenuation (see Herraiz and Espinoza (1986) for a review). Most of the developments of the theory of coda waves concern the perturbations of an homogeneous medium. This represents a severe limitation to the interpretation since the earth presents a strong vertical heterogeneity. The importance of the layering for scattered waves was investigated by Wang and Herrmann (1988) and theoretical developments in this domain remain of crucial importance for the understanding of propagation at regional distances. The most obvious effect of the stratification on the scattered field is the generation of surface waves.

Large scale shallow irregularities such as sedimentary basins also produce the local conversion of body waves into propagating surface waves (Campillo, 1987). Nevertheless, because of the large observed attenuation near the surface (Toksoz et al., 1988) and the great variability of the thickness of the surface low velocity

layer, we expect the short period surface waves to be unable to propagate along paths of several hundreds of kilometers as Pg or Lg do. Various authors have tried to numerically infer the effect of deep irregularities, such as Moho uplifts, on short period Lg (Kennett, 1984; Campillo, 1987; Maupin, 1989). Their basic conclusion is that Lg appears to be a robust and stable phase even when strong lateral variations of the crustal structure occur. In view of this result, the Lg wavetrain could be used to measure the mean attenuation in the crust. Solely, a measure of the apparent attenuation does not bring much information about the cause and the mechanism of seismic attenuation. An approach to move farther on can be to correlate the characteristics of the attenuation in different regions with the different particular crustal structures encountered. In order to avoid spurious differences that can be produced when comparing measurements made with different types of data or with different techniques, we choose to use an inversion process and a large homogeneous data set. To this end, we have to collect enough data to be able to describe the attenuation in both space and frequency domains, beneath an area sufficiently large to include different geological units.

We have obtained from the LDG seismic network a data set sufficient to cover a great part of France. We require unclipped seismograms showing an acceptable signal to noise ratio in the epicentral distance range 200-1000 km. Because of the dynamic range of the network and the modest seismicity of France this

represents long observation time. In a previous study (Campillo, 1987), we used a limited number of earthquakes (18) and of stations (22) to study a region of central France. Because of the small number of records available at that time, we applied the backprojection technique to construct a map of apparent attenuation. We shall discuss these results in a following section. In this study, we have widely increased the data set and the area studied. We will use an iterative SIRT-type reconstruction technique to determine source amplitude and quality factors. We also consider early coda of Lg and Pg waves. Gupta et al. (1989) studied the distribution of Q from Lg in eastern North America assuming a regionalization based on Bouguer gravity contours and geological maps.

### Data Processing

We selected 431 earthquakes in France and in its vicinity (Figure 1). These events were recorded at 26 short period vertical seismometers of the LDG network. Unfortunately we have never recorded simultaneously in good conditions at more than 20 stations. The records were collected during the period 1985-1987. For each record, we computed the density of spectral amplitude for four phases defined by the group velocity windows:

6.2 km/s > V > 5.6 km/s	Pg
3.6 km/s > V > 3.1 km/s	Lg1
3.1 km/s > V > 2.6 km/s	Lg2

2.6 km/s > V > 2.3 km/s Lg3

At this stage, we eliminated the traces where glitches were detected. For each record, we also computed the density of spectral amplitude of the noise in a window of 30 sec before the first arrival. For a given phase and a given frequency, the spectral density is validated if the signal to noise ratio is greater than 3.

### Data Analysis

We model the spectral amplitude observed at station j for earthquake i in the form:

$$A_{i,j}(f,d) = S_j(f) * E(d) * AA_{i,j}(f,d) * St_i(f) \quad (1)$$

where d represents the epicentral distance, f the frequency and:  
- $S_j(f)$  = the source excitation. We neglect the radiation pattern due to the focal mechanism as well as the directivity effect associated with rupture propagation. The directivity is known to be a strong effect only on wavelengths much smaller than the source dimension. The Pg and Lg wavetrains are made up of arrivals corresponding to very different take-off angles and therefore the radiation pattern is, in general very smoothed for these phases.

- $E(d)$  = the geometrical spreading of the phase considered in the time domain. After numerical investigations in flat layered models, we found (Campillo et al., 1984):

$$E(d) = d^{-0.83} \text{ for Lg}$$

and

(2)

$$E(d) = d^{-1.5} \text{ for Pg}$$

We assume in our analysis that Pg and Lg propagate mostly along straight ray paths i.e. that the mean velocity of S-waves in the crust is roughly constant. Therefore we neglect the effect of focusing-defocusing that was recognized for surface waves (e.g. Zeng et al., 1987).

$-AA_{i,j}(f,d)$  = the apparent attenuation that we express in the form:

$$AA_{i,j}(f,d) = \exp\left(-\frac{\pi f}{V} \int_d \frac{dl}{Q(f,x,y)}\right) \quad (3)$$

where  $V$  is the group velocity and  $Q$  the quality factor. This term includes the intrinsic attenuation but also other types of attenuation such as scattering, or propagation effects in a heterogeneous crust that affect the geometrical spreading.

$-ST_i(f)$  = the station response that represents the amplification due to site effects at a given station. The azimuthal dependence of the site response is neglected.

We performed data analysis, then constructed the map of the quality factor independently for each frequency. The first step of our analysis was to assume that the quality factor is constant over the area considered. Then we evaluated the mean quality

factor, the source excitation and the station response by an iterative process similar to the scheme used by Campillo et al. (1985). At first, we performed a linear regression to compute  $Q$  and  $S$  for each earthquake. When the correlation coefficient obtained is smaller than 0.8, the event is eliminated. This value allows us to remove some erroneous data that were kept after our previous sorting, but it can also lead to exclusion of data corresponding to sharp propagation anomalies. We accept this risk because we believe that the anomalous zones are well known and are located outside our study zone. In order to avoid wrong determinations of the source excitation, we use only the data for which the earthquake was recorded by at least 5 stations. An additional condition is that the difference of epicentral distance between the closest and the farthest station is larger than 40 per cent of the largest epicentral distance.

The results obtained at this stage are used as a starting model for an iterative reconstruction that will be described in the next section. The mean values of  $Q_s$  that we get from Lg are very similar to our previous results (Campillo et al., 1985) and show the same frequency dependence ( $Q_s$  varies as the square-root of the frequency). Nevertheless, the fact that we are willing to cover a large area with a dense set of paths limits the frequency range available. In fact we can work properly only with frequencies larger than 1 Hz. Figure 2 shows an example of the effective path coverage for a frequency of 3 Hz, after sorting out the data set.

### Algorithm of inversion

This algorithm is based on the use of an iterative reconstruction technique that allows us to consider large data sets on small computers. The general scheme of the complete processing is presented in Figure 3. Stage I, as denoted in Figure 3 was discussed in the last section and consists of setting up a starting model with an homogeneous  $Q(f)$ . In the next stage, we compute a set of  $Q$  values at the nodes of a regular grid to describe the actual continuous distribution of apparent attenuation.

After stage I we use equation 1, the expression for the apparent attenuation and the estimations of  $S$  and  $S_t$  to evaluate parameter  $l$ :

$$l_k = \int_{d_k} \frac{dl}{Q(f, x, y)}$$

The set of the  $l_k$ -s will be used to invert  $Q(f, x, y)$ .

The inversion techniques used are slightly modified versions of backprojection and simultaneous iterative reconstruction technique. We shall briefly describe them.

Backprojection and S.I.R.T. operate for a given unknown  $Q(f, x, y) = Q_1$  corresponding to location  $X_1 = (x, y)$  and with the data from the neighbouring paths. Following Mason (1981), we define a circle of influence around  $X_1$ . Each path contributes with a weighting coefficient proportional to its length within the circle

of influence. This approach is particularly well adapted to the present problem since we know the important part played by scattered waves and multipathing in the propagation of regional phases.

The backprojection is then slightly modified by using the expression:

$$Q_i^{-1} = \frac{\sum_{r=1}^{N_i} a_{r,i} \frac{l_r}{L_r}}{\sum_{r=1}^{N_i} a_{r,i}} \quad (4)$$

where  $N_i$  is the number of pathes that cross the circle of influence centered in  $X_i$ ,  $a_{r,i}$  is the length of the path in the circle and  $L_r$  is its total length. We compute  $Q$  values at the locations  $X_i$  for which the number of rays is larger than  $N_{min}$ . A supplementary condition is that these rays are coming from a number of distinct sources larger than  $N_{Smin}$ . When

these conditions are not satisfied, the mean value of  $Q$  is assumed. Without further precision, the results presented here are computed with  $N_{min}$  equal to 15 and  $N_{Smin}$  equal to 8.

Following Cote (1988), we implemented an iterative inversion basically derived from S.I.R.T. (Gilbert, 1972). After the  $(j-1)$ th iteration we compute the estimation of  $l$  in the  $j$ th model:  $l_r^{j-1}$ . We define the residue by:

$$res_r^j = l_r - l_r^{j-1}$$

The  $j$ th iteration consists of applying to  $Q^{-1}$  at location  $X_i$  the correction:

$$\delta(Q_1^{-1})^J = \frac{\phi(e_1)}{e_1} \sum_{r=1}^{N_1} a_{r,1} \frac{\text{res}_r^J}{L_r}$$

with:

(5)

$$e_1 = \sum_{r=1}^{N_1} a_{r,1} g_1(\theta_r)$$

and where  $\theta_r$  is the azimuth of the path  $r$  and  $f$  and  $g$  are weighting functions which we are about to describe.

$g(\theta_r)$  represents the azimuthal weighting:

$$g_1(\theta_r) = G + (1-G) (N_1 - D_1(\theta_r)) / N_1$$

where  $D_1(\theta_r)$  is the number of paths whose directions are in the range  $(\theta_r - 10^\circ, \theta_r + 10^\circ)$  and which intersect the circle of influence centered in  $X_1$ .  $G$  is a constant that controls the amplitude of the variation of the weighting and that we chose in practice equal to 0.5. The effect of  $g$  is to temperate the influence of strong heterogeneities in the distribution of rays.

The damping factor  $\phi(e_1)$  varies with the location and depends mainly on the density of rays as:

$$\phi(e_1) = R + (1-R) e_1 / e_{\max}$$

where  $e_{\max}$  is the maximum value of the cumulated weighting factors at each point computed over the entire region studied.  $R$  is a constant chosen to be equal to 0.5 in the following examples. By using a spatially dependent damping we want to limit the variations of the model in zones where the path coverage is poor. This is specially useful considering the uncertainties implied by our parametrization of the problem as will be discussed in the

next section. We have also performed tests where we added a constant to the weighting term  $e_1$ , as proposed by Comer and Clayton (1987) who suggested that this operation may stabilize the solution. In our case, this damping affects the convergence rate but has a very weak influence on the final image.

After a series of iterations to actualize the current  $Q$  model, we compute the mean residues associated with each station and each earthquake. Next, the station responses and the source excitations are corrected by terms equal to these biases multiplied by damping factors. The values of these damping factors, relative to the mean damping applied for the inversion of  $Q$  alone, can be evaluated by comparing the partial derivatives of the amplitude with respect to  $Q_1$ ,  $S$  and  $St$  in equation 1. In practice the coefficients of damping  $\epsilon_s$  and  $\epsilon_{st}$ , as well as the number of iterations on  $Q_1$  only, are chosen after numerous trials. We have studied systematically the influence of damping factors and number of internal iterations on the final misfits between model prediction and actual observations. To this aim, we repeated the inversion process tens of times with different parameters. In the following examples we have taken  $\epsilon_s$  between 0.06 and 0.04,  $\epsilon_{st}$  between 0.03 and 0.02, and the number of iterations of SIRT on  $Q_1$  only, equal to 3. With these values the complete scheme converges in about 20 iterations.

Accuracy of the results

As pointed out before, the parameters of the inversion were chosen by trial and error for the specific data set considered. After these numerical tests, it appears that applying strong damping on source excitation and station response corrections warrant the stability and the convergence of the process. The Q model obtained when the process has converged to a minimum root mean square residue is weakly sensitive to the parameters of damping used, at least when the number of data is large enough. We will illustrate the importance of reaching a critical number of data by considering independent subsets of records of phase Lg1 at a frequency of 3 Hz. We performed the inversion with 4 different sets of data. The number of sources whose records are used in the inversion are: 25, 25, 55 and 100. In the case of the 25 earthquakes subsets, we reduced  $N_{\min}$  to 8 and  $N_{S\min}$  to 3 in order to cover an area comparable to that of the other cases. The Q models obtained are presented in Figure 4. The result computed from the global data set is shown in Figure 6 (Lg1). The results obtained with the two subsets of 25 events are clearly in contradiction. On the opposite, the main features of the Q-distribution computed with the entire set of records are defined correctly when using only 55 or 100 earthquakes. We interpret this very strong dependence of the stability of the solution on the number of data by two characteristics of the technique of measurement used here. The first point concerns the representation of the term of geometrical spreading by a simple smooth functional dependence (equation 2). This is an

oversimplification even for synthetic Lg seismograms whose amplitudes exhibit large spatial fluctuations due to interferences, as shown in Campillo et al. (1984). The functional form of the spreading was defined by least squares over a large range of epicentral distance. The second point is that we make an assumption of azimuthal independence of both source excitation and site response that results in a poor precision of isolated attenuation measurements. These points explain why the measurements, and therefore the inversion reaches statistical significance only for large data sets. In our first attempt to infer the attenuation in a limited part of France through a simple backprojection (Campillo, 1987), the number of events considered was too small. Nevertheless, even if some of the maps of  $Q$  were erroneous, the general conclusions of the study are confirmed by our new results, as will be shown later.

In order to add a control on the solution obtained for the entire data set, we constructed maps of resolution computed as follows. Considering a model of  $Q_s$ ,  $S$  and  $S_t$ , we changed arbitrarily the value of  $Q_{s_1}$ , computed the new residues and operated 3 iterations of the global inversion process (that includes perturbations on source excitation and station response values). We plotted the perturbations obtained on  $Q_s$  to verify if the trade-off between the parameters results in specific unrealistic deformation of the image. We obtained a map for each location  $X_1$ . A perfectly decoupling process must produce a perturbation completely concentrated in  $X_1$ . The results obtained

are presented in Figure 5 for 6 different locations. These maps give a critical view of our results; the perturbations are far to be perfectly concentrated. Nevertheless, the perturbation occurs mostly in the region around the point considered with very small effects in remote regions. This means that we can draw a relatively optimistic conclusion: our maps are very smoothed and therefore represents a long wavelength image of the distribution of the quality factor, but on the other hand the inversion process does not produce strong spurious anomalies.

The last point that we need to discuss for an objective presentation of our results is the misfits between observed and predicted values. Our main interest in this study is the mapping of  $Q_s$ . We have seen that to infer  $Q_s$  we also need to compute source excitation and station response. Considering these two last terms as a part of our model, we can compute directly from the actual spectral amplitude an apparent  $Q_s^{-1}$  value for each record that we compare with the value predicted by the heterogeneous  $Q$  model. All misfits due to source or stations are included in this comparison. The fact that we compute the misfits directly in term of  $Q_s^{-1}$  allows to compare the amplitude of the unresolved fluctuations of the data with the amplitude of the spatial variations of  $Q_s^{-1}$  obtained from our inversion. For a frequency of 3 Hz, we found in a model with homogeneous  $Q_s^{-1}$  a standard deviation of  $8 \cdot 10^{-4}$  for a mean  $Q_s^{-1}$  of  $1.8 \cdot 10^{-3}$ . After the inversion, the standart deviation is reduced to  $4.5 \cdot 10^{-4}$ .

This indicates the significancy of the quality factor fluctuations with respect to the average misfit of the data.

#### Results obtained at 3 Hz

We have performed the inversion for the 4 time windows defined previously at the same frequency of 3 Hz. The results obtained are presented in Figure 6. The lowest Q values are reached for  $Q_p$  deduced from Pg waves. This result is somewhat surprising. As it is generally admitted that the values of intrinsic Q are larger for P waves than for S waves, another cause of apparent attenuation is required to understand this result. One possible explanation is that the Pg phase is more sensitive than the Lg phase to lateral large scale heterogeneity in the crust. This can be explained by the fact that P-waves incident on the Moho can always be refracted in the upper mantle while S-waves are trapped in the crust in a wide range of incident angle. Nevertheless, as we will see later, considering the frequency dependance will lead us to invoke the scattering in a randomly inhomogeneous medium to interpret our results. The distribution of Q inferred from Pg does not exhibit strong variations at 3 Hz. The results obtained with the records corresponding to the window Lg1 are more contrasted. The zones of high attenuation correspond to the perialpine region, the central Massif and more surprisingly an area in the North western corner of the region studied that we will identify later as the Central Armorican Zone. This example

illustrates the difficulty to base a regionalization of  $Q$  on surface geology only. We shall examine later the frequency dependence for  $Pg$  and  $Lg$ .

We also present in Figure 6 the results obtained for the windows  $Lg2$  and  $Lg3$  that correspond to the early coda of  $Lg$ . We processed and inverted these data exactly in the same way as we did for  $Lg1$ , without taking into consideration their nature of coda waves. For  $Lg2$  the image presents a clear similarity with the results obtained with  $Lg1$ . There is a slight increase of the mean value of  $Q_s$  between  $Lg1$  and  $Lg2$ . For  $Lg3$  the image is poorly resolved, although one can distinguish features which are common to  $Lg1$  and  $Lg2$ . The interpretation of the results obtained with late arrivals is difficult. Nevertheless, the very close average value of  $Q_s$  that we found from primary waves ( $Lg1$ ) and from early coda ( $Lg2$ ), assuming the same geometrical spreading for both phases suggests that these waves are associated with a only mode of propagation, as discussed in Campillo (1990).

#### Frequency dependence of $Q_s$ inferred from $Lg1$

Figure 7 presents the  $Q_s$  distributions computed at different frequencies. The images are less contrasted at high frequency in addition to the fact that, for high frequencies the contrast between quality factors with large values are much less significant in term of energy attenuation. There are two different features for the patterns shown on the figure. First

some patterns have amplitudes that vary strongly with frequency and disappear almost completely at high frequency. This can be explained by the fact that the attenuation is dominated by the effect of scattering, which is known to result in a peak of attenuation in the frequency domain. The anomalous attenuation in the Central Armorican Zone is in this first category. Otherwise, the Alpine and peri-Alpine region seems associated with attenuation whatever the frequency is, although the contrast is more significant for the lowest frequencies. This point suggests the addition of a strong intrinsic attenuation to the scattering effect in this region. Indeed there is a sedimentary basin as deep as 10 km at the western periphery of the Alpine arc. However one cannot neglect the fact that a mountain range like the Alps is associated with large scale crustal heterogeneity. This can affect the geometrical spreading of Lg and result in apparent attenuation.

One conclusion that we can draw from these images is the clear frequency dependence of the mean quality factor and the decrease in amplitude of the spatial variations of  $Q$  at high frequency. It was one of the main conclusions of a previous work (Campillo, 1987) to show that apparent attenuation in the crust occurs in a limited frequency band. This result supports the hypothesis that attenuation of crustal waves is caused mainly by scattering on small scale inhomogeneity rather than by factors producing frequency independent effects such as inelasticity or large scale lateral heterogeneity. The distribution of  $Q$  follows

the trend towards associating tectonically active regions with low  $Q$ . But an intriguing problem is , for frequencies between 2 and 8 Hz, the existence of a region of high attenuation beneath the Hercynian basement of western France.

#### Frequency dependence of $Q_p$ inferred from $P_g$

The results obtained for  $Q_p$  at 4 different frequencies are presented in Figure 8. The image obtained at 2 Hz is shown only to illustrate the strong frequency dependence of  $Q_p$  in this frequency range. Actually  $Q_p$  varies with frequency even faster than  $Q_s$ . There is a relatively good agreement between the patterns obtained for  $Q_p$  and  $Q_s$ , although the images obtained for  $Q_p$  are less contrasted. This seems to indicate that, in spite of the different absolute values obtained for  $Q_s$  and  $Q_p$ , the causes of attenuation are the same for the two types of waves.

#### Discussion of the mean values of apparent $Q_s$

$Q_p$  inferred from  $P_g$  is smaller than  $Q_s$  obtained from  $Lg_1$  over the whole frequency range. We can interpret both apparent attenuations in terms of intrinsic attenuation and scattering effect. If we consider the mean values of the quality factors we find that the frequency dependence is stronger for  $Q_p$  than for  $Q_s$ . As this is also true for the different regions we will discuss only the results obtained for the mean values. This does not mean

that the inversion is useless, on the contrary it allows a better evaluation of source excitations and station responses and therefore a more accurate measurement of  $Q$ .

The frequency dependence cannot be directly analyzed because anelasticity and scattering are both acting with a priori unknown strength. In fact we can make reasonable assumptions about the frequency dependence of these two terms. Intrinsic  $Q$  has a high value with a very weak frequency dependence as found from measurements in shield areas (Nuttli, 1982; Singh and Herrmann, 1983; Hasegawa, 1985). Sato (1984), under a single scattering assumption, predicted that scattering  $Q$  varies with the frequency for wavelengths smaller than the correlation distance. In the same paper Sato showed that his theoretical results are in agreement with the observations made in different active regions. Assuming that we deal with wavelength smaller than the correlation distance, Sato's results indicate that the scattering  $Q$  is expected to be larger for S waves than for P waves and it is effectively our observation. We have subtracted from our results the effect of the intrinsic attenuation that we consider to be represented by a constant  $Q$  of 1500. After this correction we find  $Q_s^{\text{scatt}}$  and  $Q_p^{\text{scatt}}$  to be proportional to the frequency in the range 2 Hz-10 Hz as shown in Figure 9. The ratio between quality factors of S and P waves (about 1.5) is not as large as predicted by Sato (1984): 2.41. If we assume a correlation distance of 2 km, our results indicate a mean fluctuation of 5% when measured from S waves and of 4% when measured from P waves.

These values are actually very close. One can remember that this simple interpretation is done under the assumption that the entire path of the wave is within the randomly inhomogeneous medium. These values can be underestimated if it appears that only a part of the crust is concerned by the scattering. We can conclude from the mean values of the quality factor that there is a good agreement between our experimental results and the theoretical predictions drawn by Sato within the mean wave formalism framework.

#### Discussion of the spatial distribution of apparent attenuation

We have discussed our results in terms of average values for the entire area and the whole depth of the crust. We may now try to understand the distribution of the apparent quality factor. One of the main features of our image is the attenuative character of the Alpine region. Nevertheless we have seen that the poor resolution of our inversion in this area that does not allow a detailed analysis of this very complex region. It is a well known observation that active mountain ranges are associated with low  $Q$ . A more puzzling feature is the existence of a region of attenuating material elongated in the direction NW-SE in the north-western part of France. This pattern is neither correlated with the surface geology nor with the distribution of seismicity (Figure 1 gives a realistic view of the seismicity). The direction of elongation corresponds to the structural direction of

the Variscan basement in this region (Matte and Hirn, 1988). The deep crustal structures are known in this region since the "ECORS Nord de la France" experiment which consisted of a vertical reflection seismic profile and of a wide angle profile. The records obtained with this last technique have been interpreted by Matte and Hirn (1988). Their profile crosses the low Q region that we found in northwestern France. This is a very fortunate opportunity to compare the apparent attenuation of the crust in a given region with its heterogeneity as revealed by seismic exploration. The part of the seismic section that corresponds to the intersection with the zone of higher attenuation is characterized by a very specific seismic signature as shown in Figure 10. This zone is bounded by two faults that seem to cross the entire crust. The reflections from the lower crust are numerous and have large amplitudes, indicating strong impedance contrasts. This comparison between the image produced by seismic reflection experiment and the apparent attenuation supports the hypothesis that scattering plays an important part in the attenuation of seismic waves within the crust. Indeed this agreement may be fortuitous but it is the only example of such a comparison that we can make with our data set.

An interesting feature of this comparison is that it indicates a correlation between the apparent attenuation of multiply reflected crustal waves and the heterogeneity of the lower crust. The heterogeneity of the lower crust is revealed by its large reflectivity in most of the examples of deep reflexion

profiles (e.g. Brown et al., 1986; Peddy and Hobbs, 1987). On the contrary the upper crust is generally more transparent to seismic waves. The strong scattering of short period waves in the crust could be localized in the region of strong reflectivity, i.e. the lower crust. A controversial hypothesis can be drawn: most of the attenuation occurs in two regions of the crust: the first few kilometers beneath the surface as suggested by Toksoz et al. (1988) and the highly inhomogeneous lower crust as shown in our study. The fact that an important part of apparent attenuation of S waves originates in the possibly ductile lower crust is consistent with the explanation of the temporal variation of coda Q proposed by Jin and Aki (1989).

### Conclusion

We have shown that a precise measurement of  $Q_s$  or  $Q_p$  from regional phase records requires the processing of a large data set. The very large trade-off between the unknowns necessitates a very careful interpretation of the results of the inversion. We believe that the inversion may be also useful to increase the accuracy of the measurement of the mean value of the quality factors. We have shown that the relatively poor resolution of our inversion results in an important smoothing of the image but does not produce artefacts.

The results obtained show the frequency dependance of  $Q_p$  and  $Q_s$ . A simple analysis shows that the mean values obtained are in

agreement with the single scattering model of Sato (1984) which implies a linear dependence of the quality factor with frequency and larger values of  $Q_p$  than  $Q_s$ . We found that the mean fluctuation of velocity needed to explain the data is about 5%. The distribution of quality factors is governed by large scale structures such as the alpine range. We found that ancient structures can be associated with zones of high attenuation. The Central American Zone in the Variscan belt is an example of that. Because we have an image of the crustal structure obtained with wide angle reflexion, we can associate the high apparent attenuation in this zone with scattering in a highly heterogeneous lower crust. Such a comparison between the apparent attenuation and the observed heterogeneity of the crust must be repeated to confirm the correlation obtained in this paper. The quality factor tomography is useful for the quantitative interpretation of short period seismic phases but if such a correlation is confirmed, it can also be a promising tool of investigation of deep crustal structures.

#### AKNOWLEDGMENTS

This work was supported by the Advanced Research Projects Agency and was monitored by the Air Force Office of Scientific Research under Grant 87.0331.

#### REFERENCES

Aki, K. 1969 Analysis of the seismic coda of local earthquakes as

scattered waves. J. Geophys. Res. 74, 615-631.

Brown, L., M. Barazangi, S. Kaufman and J. Oliver 1986 The first decade of COCORP 1974-1984 in "Reflection Seismology: a global perspective", edited by M. Barazangi and L. Brown, AGU Geodyn. Series 13, 107-120.

Campillo, M. 1987 Lg wave propagation in a laterally varying crust and the distribution of quality factor in Central France. J. Geophys. Res. 92, 12604-12614.

Campillo, M. 1990 Propagation and attenuation characteristics of the crustal phase Lg. Pure Appl. Geophys. 132

Campillo, M., M. Bouchon and B. Massinon 1984 Theoretical study of the excitation, spectral characteristics and geometrical attenuation of regional seismic phases. Bull. Seism. Soc. Am. 74, 79-90.

Campillo, M., J.L. Plantet and M. Bouchon 1985 Frequency dependent attenuation in the crust beneath Central France from Lg waves: data analysis and numerical modelling. Bull. Seism. Soc. Am. 75, 1395-1411.

Comer, R.P. and R.W. Clayton 1987 Reconstruction of mantle heterogeneity by iterative back-projection of travel times I

Theory and reliability. J.G.R

Cote, P 1988 Tomographies sismiques en genie civil, PhD Thesis, Universite Joseph Fourier, Grenoble, France

Gilbert, P. 1972 Iterative Methods for the three dimensional reconstruction of an object from projections. J. theor. Biol 36, 105-117.

Gupta, I.N., K.L. McLaughlin, R.A. Wagner, R.S. Jih and T.W. McElfresh, 1989 Seismic wave attenuation in eastern North America, EPRI RP 2556-9 final report, EPRI, Palo Alto, Ca.

Hasegawa, H.S. 1985 Attenuation of Lg waves in the Canadian shield. Bull. Seism. Soc. Am. 75, 1569-1582.

Herraiz, M. and A.F. Espinoza 1986 Scattering and attenuation of high frequency seismic waves: development of the theory of coda waves. USGS Open-File Report 86-455.

JIN, A. and K. Aki 1989 Spatial and temporal correlation between coda  $Q^{-1}$  and seismicity and its physical mechanism, in press J. Geophys. Res.

Kennett, B.L.N. 1984 Guided wave propagation in laterally varying media, I, Theoretical development, Geophys. J. R. Astr. Soc. 79,

235-255.

Mason, I.M. 1981 Algebraic reconstruction of two-dimensional velocity inhomogeneity in the High Hazles seam of Thoresby colliery. *Geophysics* 46, 298-308.

Matte, P. and A. Hirn 1988 Seismic signature and tectonic cross section of the Variscan crust, *Tectonics* 7, 141-155.

Maupin, V 1989 Numerical modelling of Lg propagation across the North Sea central graben, *Geophys. J.* in press

Nuttli, O. 1973 Seismic wave attenuation and magnitude relations for eastern North America, *J. Geophys. Res.* 78, 876-885.

Nuttli, O. 1982 The earthquake problem in the eastern United States, *J. Struct. Div. Am. Soc. Civ. Eng.* 108, 1302-1312.

Nuttli, O. 1986 Yield estimates of Nevada Test Site explosions obtained from seismic Lg waves, *J. Geophys. Res.* 91, 2137-2151.

Peddy, C.P. and R.W. Hobbs 1987 Lower crustal reflectivity of the continental margin Southwest of Britain. *Annales Geophysicae* B5, 331-338

Sato, H. 1984 Attenuation and envelope formation of

three-component seismograms of small local earthquakes in randomly inhomogeneous lithosphere. J. Geophys. Res. 89, 1221-1241.

Singh, S.K. and R.B. Herrmann 1983 Regionalization of crustal coda Q in the continental United States, J. Geophys. Res. 88, 527-538.

Toksoz, M.N., A. Dainty, E. Reuter and R.S. Wu 1988 A model for attenuation and scattering in the earth's crust. Pure Appl. Geophys. 128, 81-101.

Wang, C.Y. and R.B. Herrmann 1988 Synthesis of coda waves in layered medium. Pure Appl. Geophys. 128, 7-42.

Zeng, Y.H., J. Faulkner, T.L. Teng and K. Aki 1987 Focusing and defocusing of Rayleigh waves from USSR across arctic region to US. EOS Trans. AGU, 68, 1377.

#### Figure Captions

Figure 1: Locations of earthquakes (squares) and stations (black dots) used in this study.

Figure 2: Path coverage at a frequency of 3 Hz.

Figure 3: Scheme of data processing and inversion.

Figure 4: Results obtained with different subsets of 25, 25, 55 and 100 events.

Figure 5: Resolution maps relative to 6 different locations.

Figure 6: Results obtained at 3 Hz for the 4 group velocity windows considered.

Figure 7: Results obtained for the group velocity window Lg1 at different frequencies.

Figure 8: Results obtained for Qp in the group velocity window corresponding to Pg

Figure 9: Frequency dependence of the quality factor for P and S waves after correction of our result from a frequency independent intrinsic Q of 1500.

Figure 10: Wide angle reflection profile showing a zone of strong heterogeneity in the crust (after Matte and Hirn, 1988) and the apparent Qs inferred from Lg (Lg1).

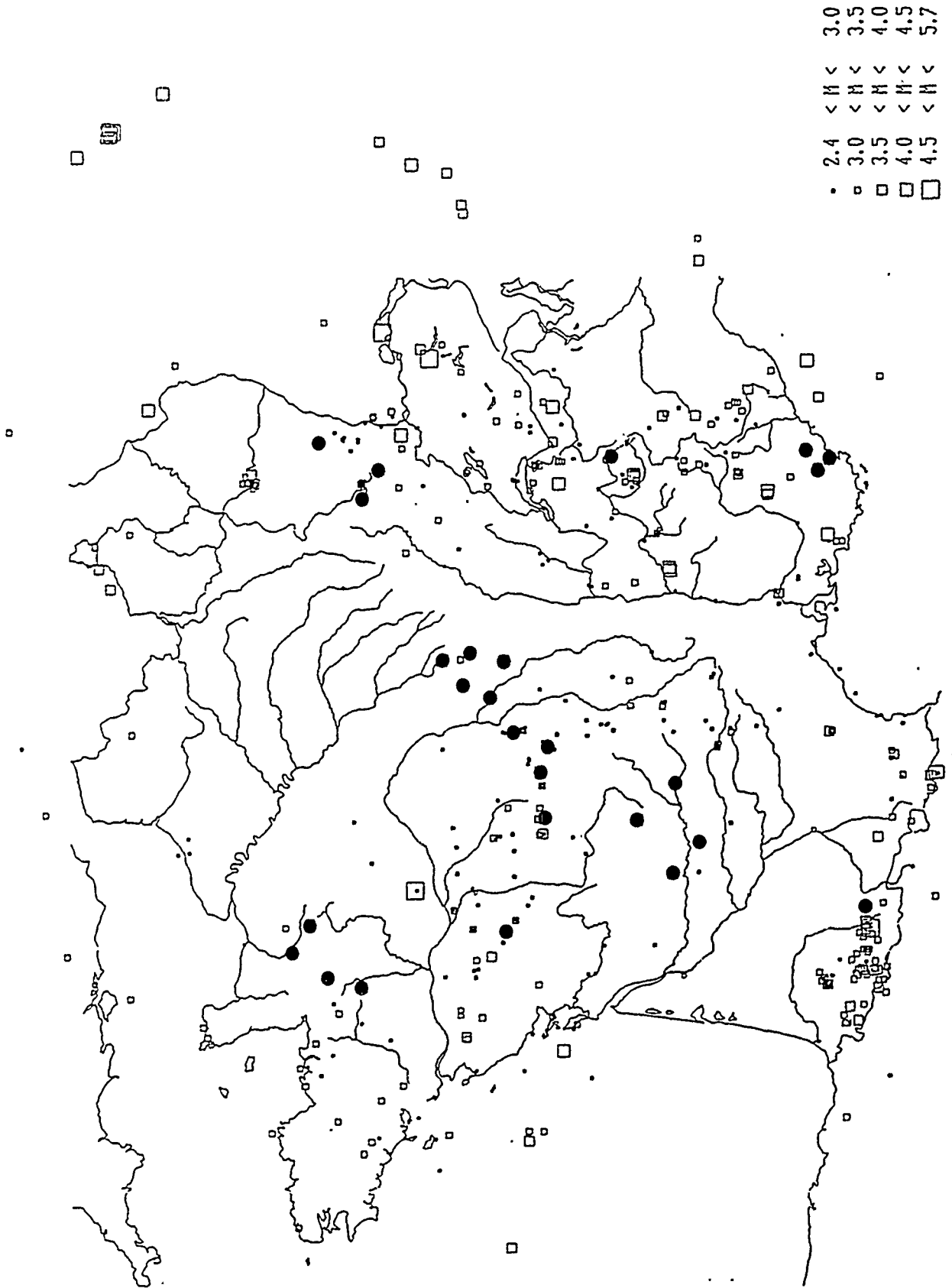


FIGURE I



FIGURE 2

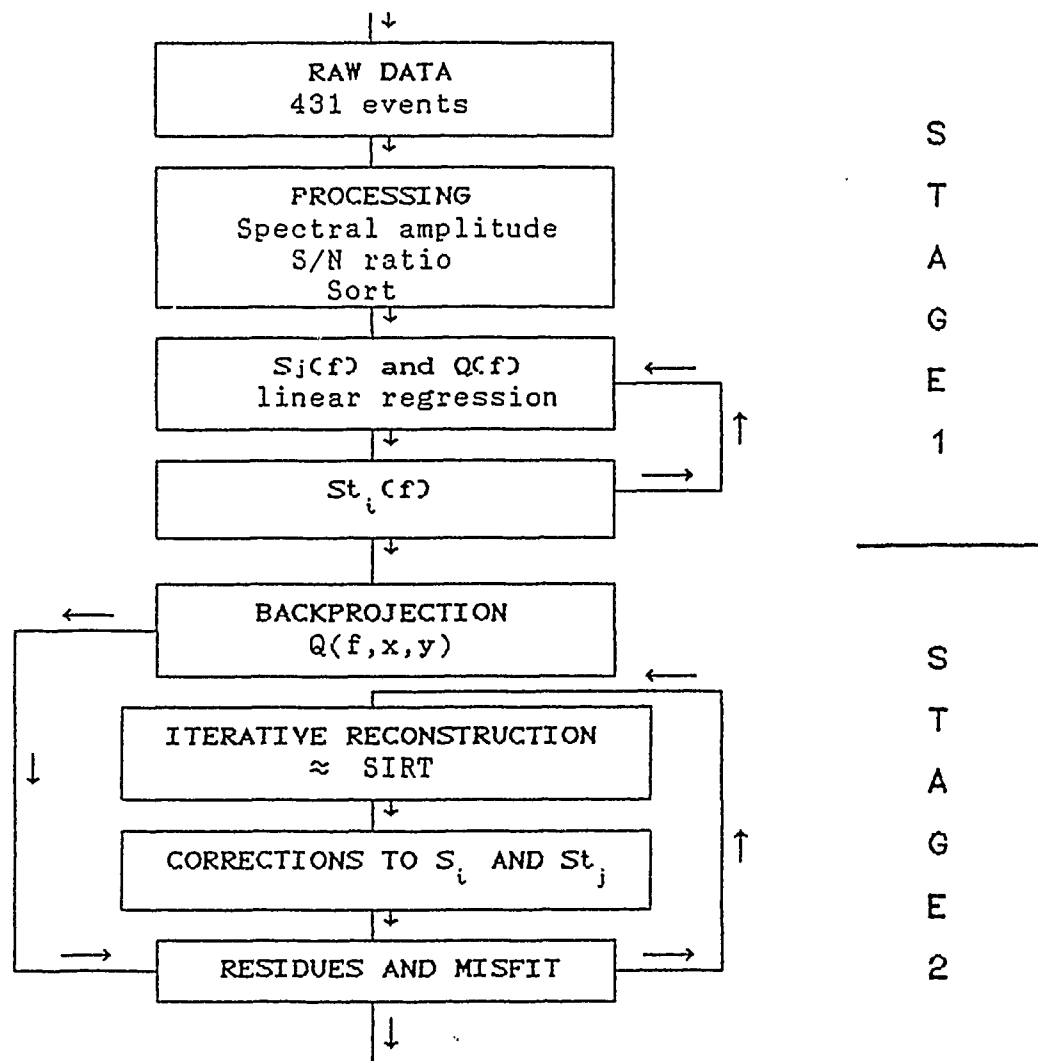


FIGURE 3

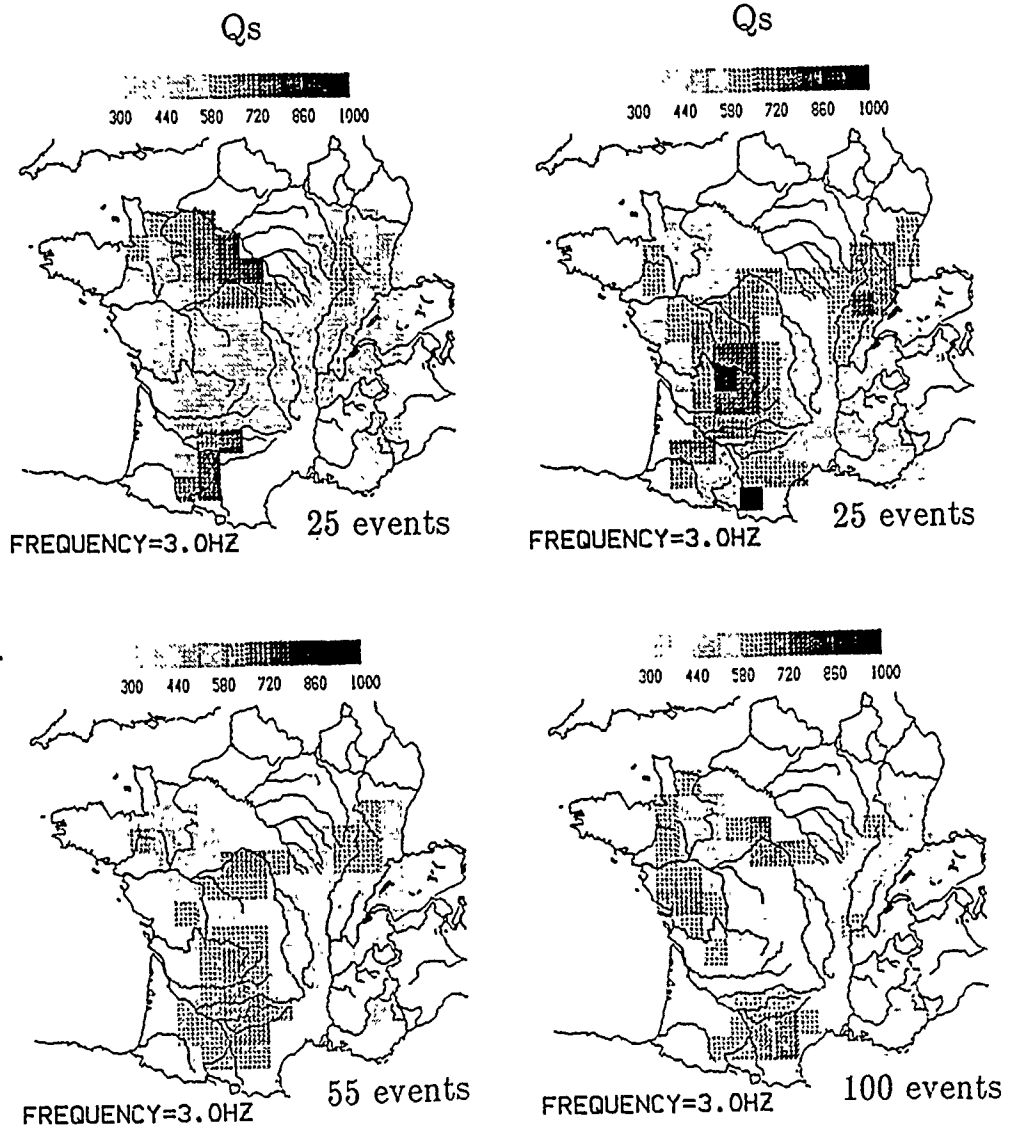


FIGURE 4

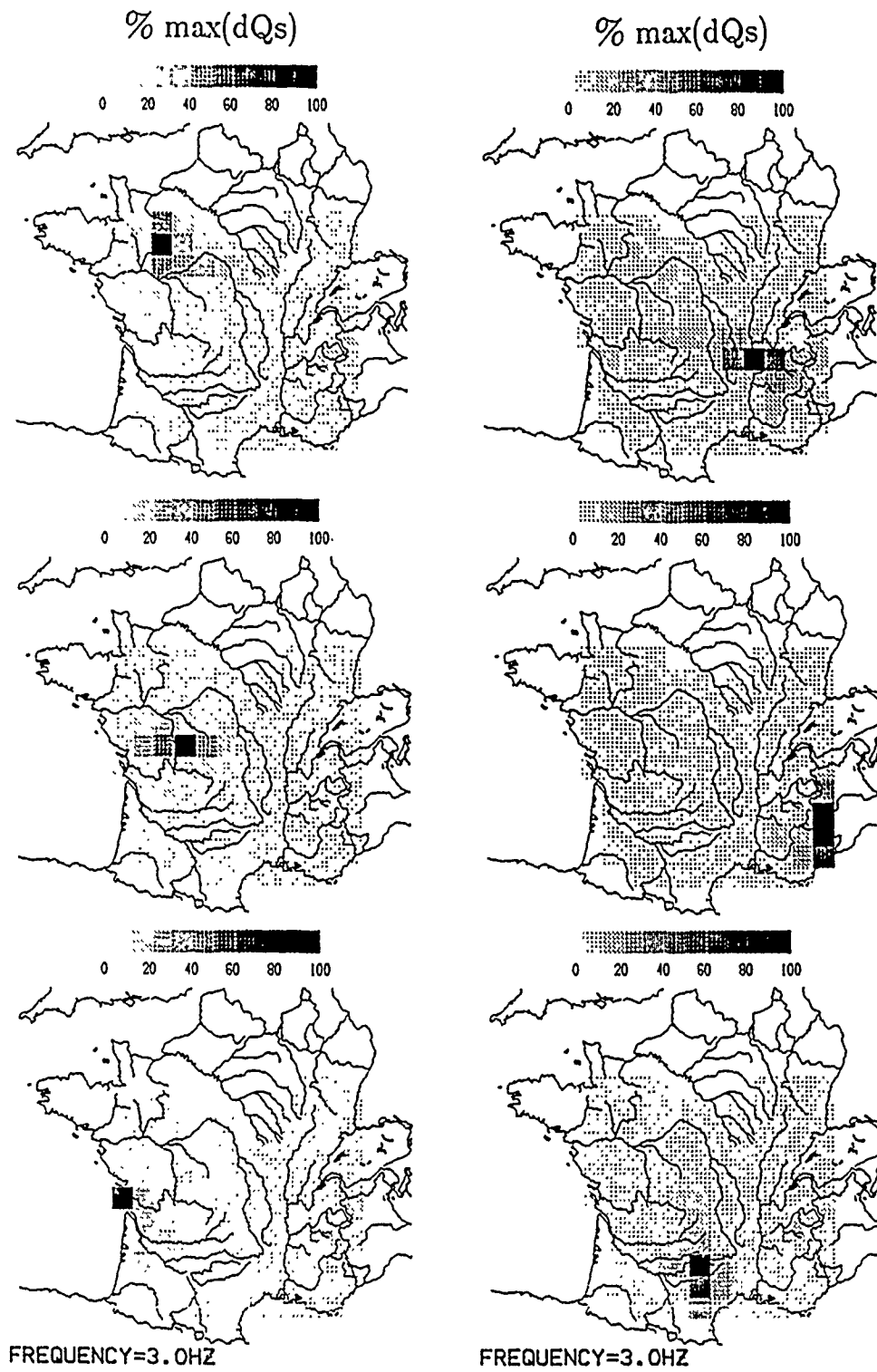


FIGURE 5

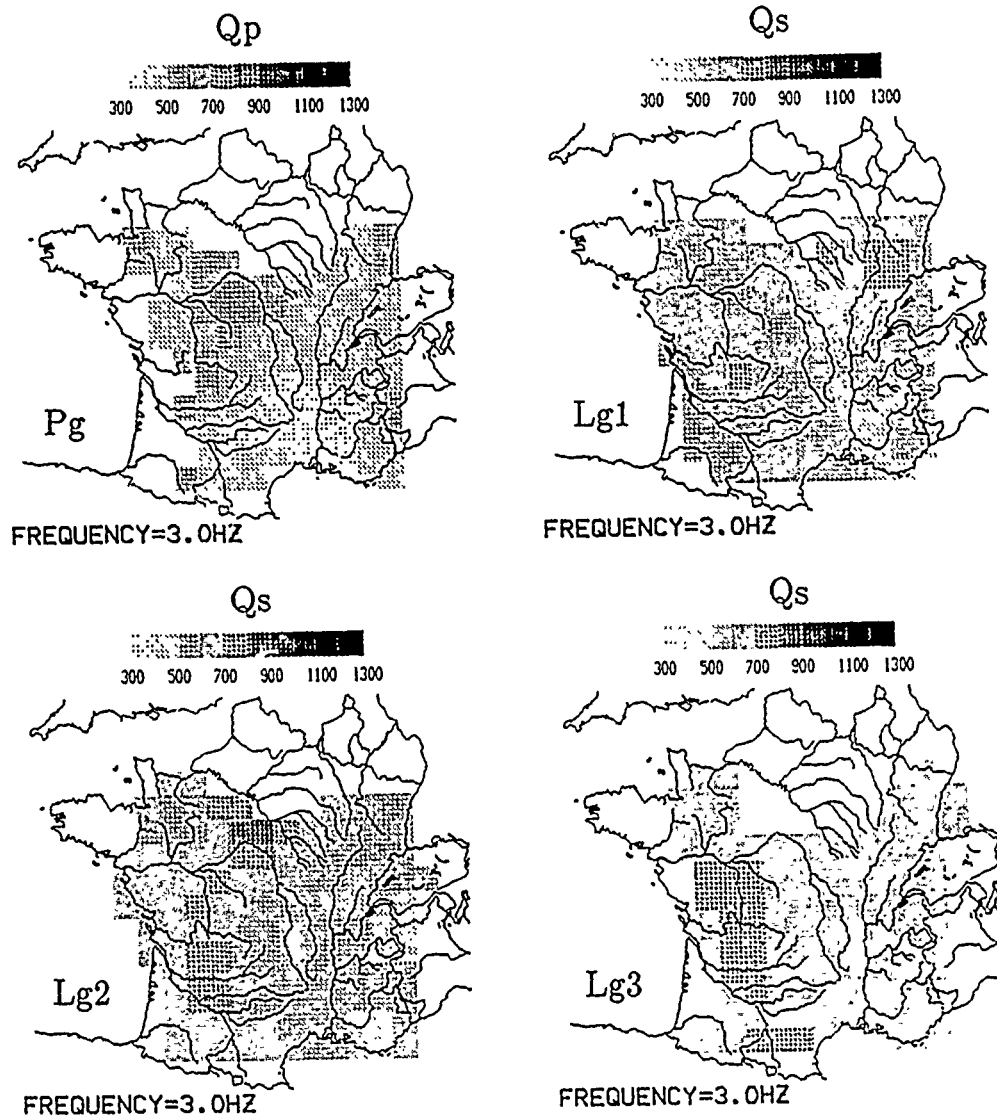


FIGURE 6

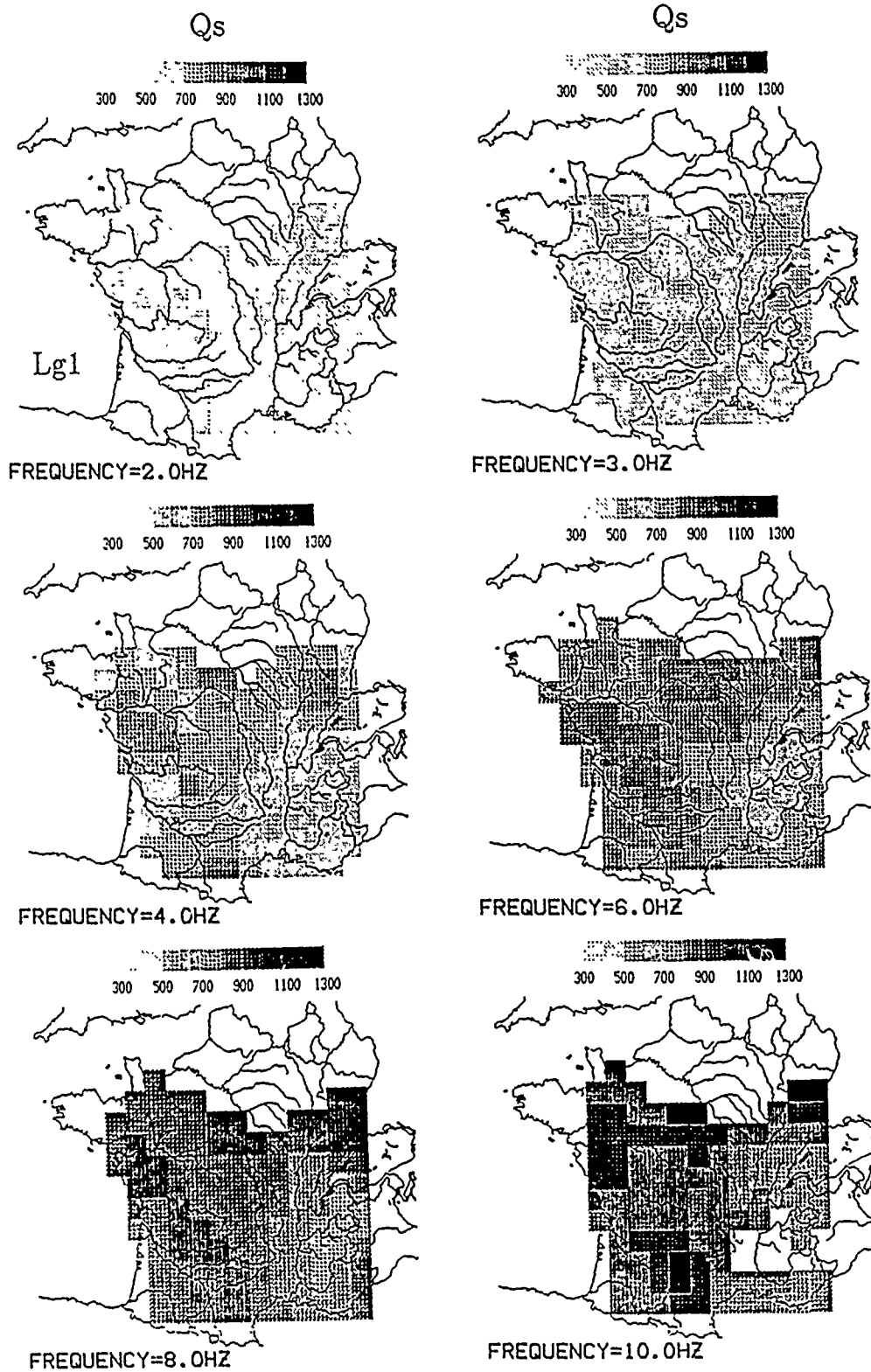


FIGURE 7

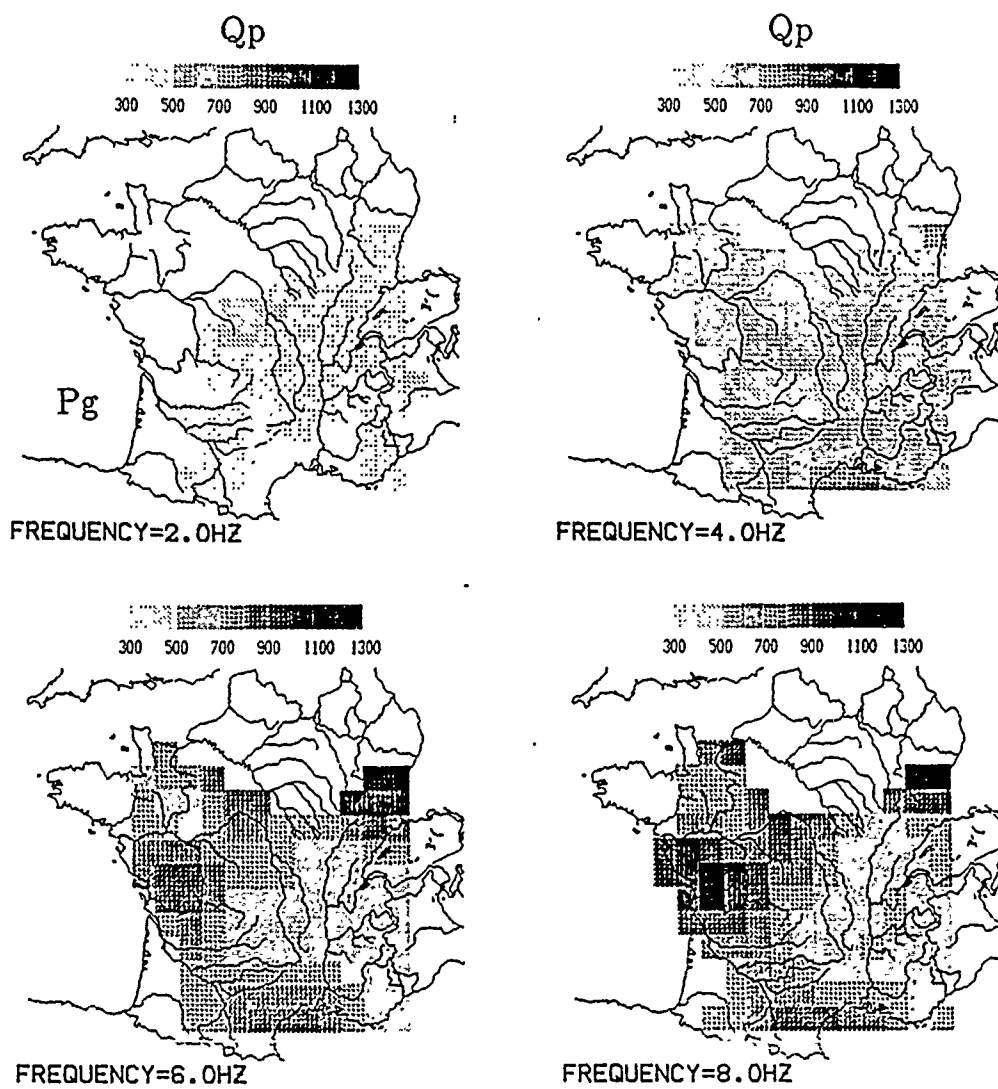


FIGURE 8

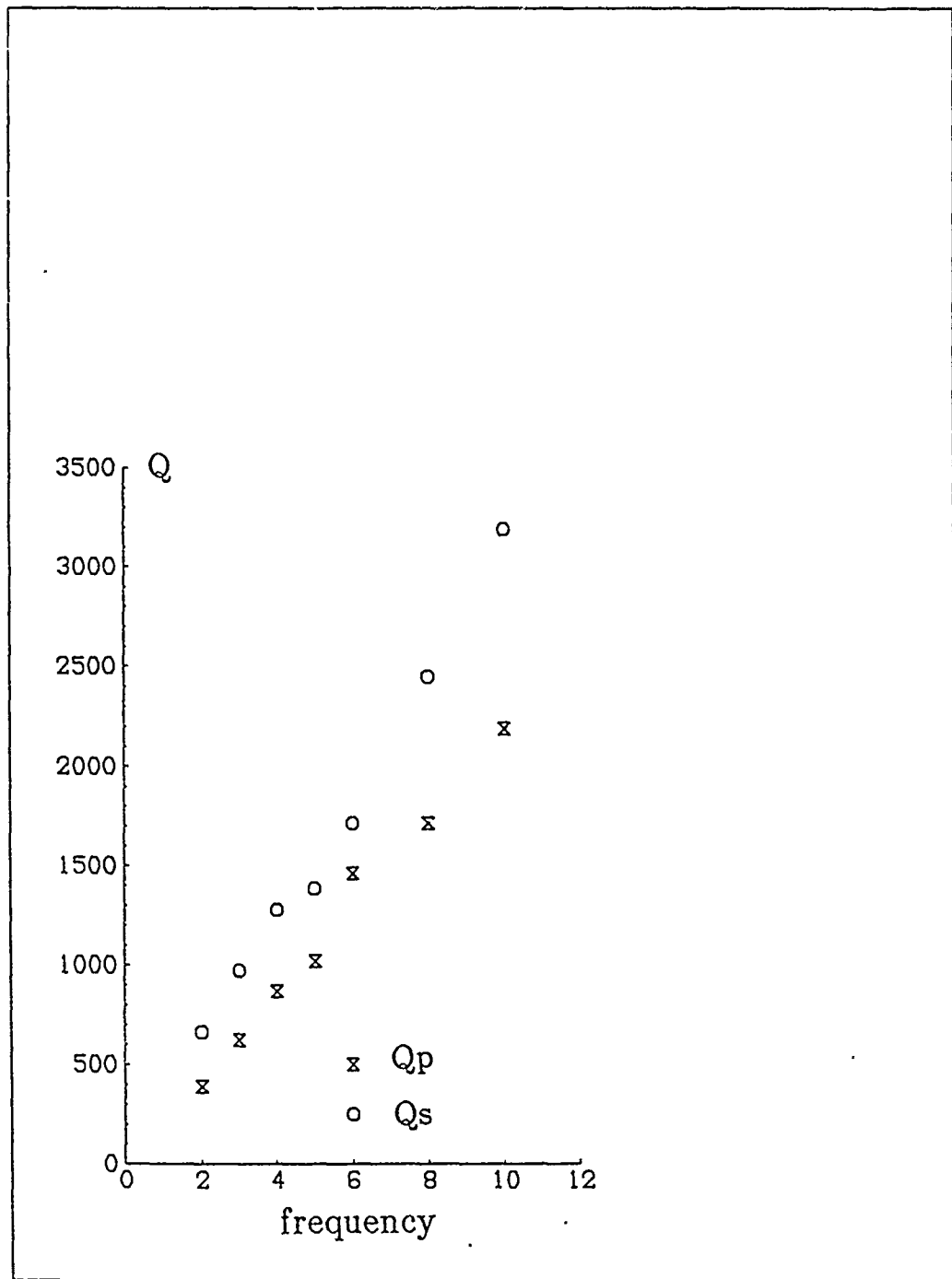


FIGURE 9

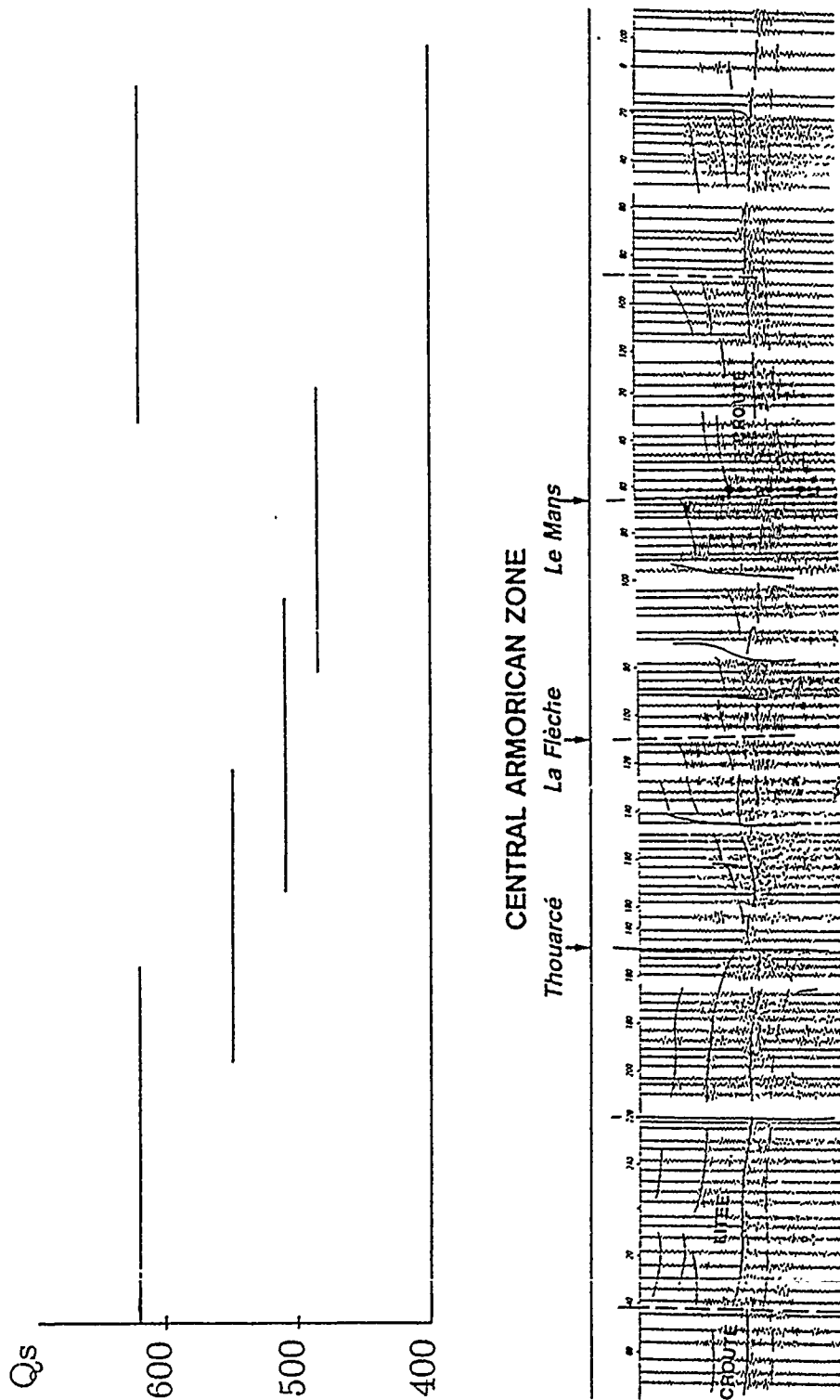


FIGURE 10

Contractors (United States)

Prof. Thomas Ahrens  
Seismological Lab, 252-21  
Division of Geological & Planetary Sciences  
California Institute of Technology  
Pasadena, CA 91125

Prof. Charles B. Archambeau  
CIRES  
University of Colorado  
Boulder, CO 80309

Prof. Muawia Barazangi  
Institute for the Study of the Continent  
Cornell University  
Ithaca, NY 14853

Dr. Douglas R. Baumgardt  
ENSCO, Inc  
5400 Port Royal Road  
Springfield, VA 22151-2388

Prof. Jonathan Berger  
IGPP, A-025  
Scripps Institution of Oceanography  
University of California, San Diego  
La Jolla, CA 92093

Dr. Lawrence J. Burdick  
Woodward-Clyde Consultants  
566 El Dorado Street  
Pasadena, CA 91109-3245

Dr. Karl Coyner  
New England Research, Inc.  
76 Olcott Drive  
White River Junction, VT 05001

Prof. Vernon F. Cormier  
Department of Geology & Geophysics  
U-45, Room 207  
The University of Connecticut  
Storrs, CT 06268

Professor Anton W. Dainty  
Earth Resources Laboratory  
Massachusetts Institute of Technology  
42 Carleton Street  
Cambridge, MA 02142

Prof. Steven Day  
Department of Geological Sciences  
San Diego State University  
San Diego, CA 92182

Dr. Zoltan A. Der  
ENSCO, Inc.  
5400 Port Royal Road  
Springfield, VA 22151-2388

Prof. John Ferguson  
Center for Lithospheric Studies  
The University of Texas at Dallas  
P.O. Box 830688  
Richardson, TX 75083-0688

Prof. Stanley Flatte  
Applied Sciences Building  
University of California  
Santa Cruz, CA 95064

Dr. Alexander Florence  
SRI International  
333 Ravenswood Avenue  
Menlo Park, CA 94025-3493

Prof. Henry L. Gray  
Vice Provost and Dean  
Department of Statistical Sciences  
Southern Methodist University  
Dallas, TX 75275

Dr. Indra Gupta  
Teledyne Geotech  
314 Montgomery Street  
Alexandria, VA 22314

Prof. David G. Harkrider  
Seismological Laboratory  
Division of Geological & Planetary Sciences  
California Institute of Technology  
Pasadena, CA 91125

Prof. Donald V. Helmberger  
Seismological Laboratory  
Division of Geological & Planetary Sciences  
California Institute of Technology  
Pasadena, CA 91125

Prof. Eugene Herrin  
Institute for the Study of Earth and Man  
Geophysical Laboratory  
Southern Methodist University  
Dallas, TX 75275

Prof. Robert B. Herrmann  
Department of Earth & Atmospheric Sciences  
St. Louis University  
St. Louis, MO 63156

Prof. Bryan Isacks  
Cornell University  
Department of Geological Sciences  
SNEE Hall  
Ithaca, NY 14850

Dr. Rong-Song Jih  
Teledyne Geotech  
314 Montgomery Street  
Alexandria, VA 22314

Prof. Lane R. Johnson  
Seismographic Station  
University of California  
Berkeley, CA 94720

Prof. Alan Kafka  
Department of Geology & Geophysics  
Boston College  
Chestnut Hill, MA 02167

Dr. Richard LaCoss  
MIT-Lincoln Laboratory  
M-200B  
P. O. Box 73  
Lexington, MA 02173-0073 (3 copies)

Prof Fred K. Lamb  
University of Illinois at Urbana-Champaign  
Department of Physics  
1110 West Green Street  
Urbana, IL 61801

Prof. Charles A. Langston  
Geosciences Department  
403 Deike Building  
The Pennsylvania State University  
University Park, PA 16802

Prof. Thorne Lay  
Institute of Tectonics  
Earth Science Board  
University of California, Santa Cruz  
Santa Cruz, CA 95064

Prof. Arthur Lerner-Lam  
Lamont-Doherty Geological Observatory  
of Columbia University  
Palisades, NY 10964

Dr. Christopher Lynnes  
Teledyne Geotech  
314 Montgomery Street  
Alexandria, VA 22314

Prof. Peter Malin  
University of California at Santa Barbara  
Institute for Crustal Studies  
Santa Barbara, CA 93106

Dr. Randolph Martin, III  
New England Research, Inc.  
76 Olcott Drive  
White River Junction, VT 05001

Dr. Gary McCartor  
Mission Research Corporation  
735 State Street  
P.O. Drawer 719  
Santa Barbara, CA 93102 (2 copies)

Prof. Thomas V. McEvelly  
Seismographic Station  
University of California  
Berkeley, CA 94720

Dr. Keith L. McLaughlin  
S-CUBED  
A Division of Maxwell Laboratory  
P.O. Box 1620  
La Jolla, CA 92038-1620

Prof. William Menke  
Lamont-Doherty Geological Observatory  
of Columbia University  
Palisades, NY 10964

Stephen Miller  
SRI International  
333 Ravenswood Avenue  
Box AF 116  
Menlo Park, CA 94025-3493

Prof. Bernard Minster  
IGPP, A-025  
Scripps Institute of Oceanography  
University of California, San Diego  
La Jolla, CA 92093

Prof. Brian J. Mitchell  
Department of Earth & Atmospheric Sciences  
St. Louis University  
St. Louis, MO 63156

Mr. Jack Murphy  
S-CUBED, A Division of Maxwell Laboratory  
11800 Sunrise Valley Drive  
Suite 1212  
Reston, VA 22091 (2 copies)

Dr. Bao Nguyen  
GL/LWH  
Hanscom AFB, MA 01731-5000

Prof. John A. Orcutt  
IGPP, A-025  
Scripps Institute of Oceanography  
University of California, San Diego  
La Jolla, CA 92093

Prof. Keith Priestley  
University of Cambridge  
Bullard Labs, Dept. of Earth Sciences  
Madingley Rise, Madingley Rd.  
Cambridge CB3 0EZ, ENGLAND

Prof. Paul G. Richards  
L-210  
Lawrence Livermore National Laboratory  
Livermore, CA 94550

Dr. Wilmer Rivers  
Teledyne Geotech  
314 Montgomery Street  
Alexandria, VA 22314

Prof. Charles G. Sammis  
Center for Earth Sciences  
University of Southern California  
University Park  
Los Angeles, CA 90089-0741

Prof. Christopher H. Scholz  
Lamont-Doherty Geological Observatory  
of Columbia University  
Palisades, NY 10964

Prof. David G. Simpson  
Lamont-Doherty Geological Observatory  
of Columbia University  
Palisades, NY 10964

Dr. Jeffrey Stevens  
S-CUBED  
A Division of Maxwell Laboratory  
P.O. Box 1620  
La Jolla, CA 92038-1620

Prof. Brian Stump  
Institute for the Study of Earth & Man  
Geophysical Laboratory  
Southern Methodist University  
Dallas, TX 75275

Prof. Jeremiah Sullivan  
University of Illinois at Urbana-Champaign  
Department of Physics  
1110 West Green Street  
Urbana, IL 61801

Prof. Clifford Thurber  
University of Wisconsin-Madison  
Department of Geology & Geophysics  
1215 West Dayton Street  
Madison, WI 53706

Prof. M. Nafi Toksoz  
Earth Resources Lab  
Massachusetts Institute of Technology  
42 Carleton Street  
Cambridge, MA 02142

Prof. John E. Vidale  
University of California at Santa Cruz  
Seismological Laboratory  
Santa Cruz, CA 95064

Prof. Terry C. Wallace  
Department of Geosciences  
Building #77  
University of Arizona  
Tucson, AZ 85721

Dr. Raymond Willeman  
GL/LWH  
Hanscom AFB, MA 01731-5000

Dr. Lorraine Wolf  
GL/LWH  
Hanscom AFB, MA 01731-5000

Prof. Francis T. Wu  
Department of Geological Sciences  
State University of New York  
at Binghamton  
Vestal, NY 13901

OTHERS (United States)

Dr. Monem Abdel-Gawad  
Rockwell International Science Center  
1049 Camino Dos Rios  
Thousand Oaks, CA 91360

Prof. Keiiti Aki  
Center for Earth Sciences  
University of Southern California  
University Park  
Los Angeles, CA 90089-0741

Prof. Shelton S. Alexander  
Geosciences Department  
403 Deike Building  
The Pennsylvania State University  
University Park, PA 16802

Dr. Kenneth Anderson  
BBNSTC  
Mail Stop 14/1B  
Cambridge, MA 02238

Dr. Ralph Archuleta  
Department of Geological Sciences  
University of California at Santa Barbara  
Santa Barbara, CA 93102

Dr. Thomas C. Bache, Jr.  
Science Applications Int'l Corp.  
10210 Campus Point Drive  
San Diego, CA 92121 (2 copies)

J. Barker  
Department of Geological Sciences  
State University of New York  
at Binghamton  
Vestal, NY 13901

Dr. T.J. Bennett  
S-CUBED  
A Division of Maxwell Laboratory  
11800 Sunrise Valley Drive, Suite 1212  
Reston, VA 22091

Mr. William J. Best  
907 Westwood Drive  
Vienna, VA 22180

Dr. N. Biswas  
Geophysical Institute  
University of Alaska  
Fairbanks, AK 99701

Dr. G.A. Bollinger  
Department of Geological Sciences  
Virginia Polytechnical Institute  
21044 Derring Hall  
Blacksburg, VA 24061

Dr. Steven R. Bratt  
Center for Seismic Studies  
1700 North 17th St., Suite 1450  
Arlington, VA 22209

Michael Browne  
Teledyne Geotech  
3401 Shiloh Road  
Garland, TX 75041

Mr. Roy Burger  
1221 Serry Road  
Schenectady, NY 12309

Dr. Robert Burrige  
Schlumberger-Doll Research Center  
Old Quarry Road  
Ridgefield, CT 06877

Dr. Jerry Carter  
Rondout Associates  
P.O. Box 224  
Stone Ridge, NY 12484

Dr. W. Winston Chan  
Teledyne Geotech  
314 Montgomery Street  
Alexandria, VA 22314-1581

Dr. Theodore Cherry  
Science Horizons, Inc.  
710 Encinitas Blvd., Suite 200  
Encinitas, CA 92024 (2 copies)

Prof. Jon F. Claerbout  
Department of Geophysics  
Stanford University  
Stanford, CA 94305

Prof. Robert W. Clayton  
Seismological Laboratory  
Division of Geological & Planetary Sciences  
California Institute of Technology  
Pasadena, CA 91125

Prof. F. A. Dahlen  
Geological and Geophysical Sciences  
Princeton University  
Princeton, NJ 08544-0636

Dr. Jeffrey W. Given  
Sierra Geophysics  
11255 Kirkland Way  
Kirkland, WA 98033

• Prof. Adam Dziewonski  
Hoffman Laboratory  
Harvard University  
20 Oxford St  
\* Cambridge, MA 02138

Prof. Stephen Grand  
University of Texas at Austin  
Department of Geological Sciences  
Austin, TX 78713-7909

Prof. John Ebel  
Department of Geology & Geophysics  
Boston College  
Chestnut Hill, MA 02167

Prof. Roy Greenfield  
Geosciences Department  
403 Deike Building  
The Pennsylvania State University  
University Park, PA 16802

Eric Fielding  
SNEE Hall  
INSTOC  
Cornell University  
Ithaca, NY 14853

Dan N. Hagedorn  
Battelle  
Pacific Northwest Laboratories  
Batteile Boulevard  
Richland, WA 99352

Prof. Donald Forsyth  
Department of Geological Sciences  
Brown University  
Providence, RI 02912

Kevin Hutchenson  
Department of Earth Sciences  
St. Louis University  
3507 Laclede  
St. Louis, MO 63103

Dr. Cliff Frolich  
Institute of Geophysics  
8701 North Mopac  
Austin, TX 78759

Prof. Thomas H. Jordan  
Department of Earth, Atmospheric  
and Planetary Sciences  
Massachusetts Institute of Technology  
Cambridge, MA 02139

Prof. Art Frankel  
Mail Stop 922  
Geological Survey  
790 National Center  
Reston, VA 22092

Robert C. Kemerait  
ENSCO, Inc.  
445 Pineda Court  
Melbourne, FL 32940

Dr. Anthony Gangi  
Texas A&M University  
Department of Geophysics  
College Station, TX 77843

William Kikendall  
Teledyne Geotech  
3401 Shiloh Road  
Garland, TX 75041

• Dr. Freeman Gilbert  
Inst. of Geophysics & Planetary Physics  
University of California, San Diego  
\* P.O. Box 109  
La Jolla, CA 92037

Prof. Leon Knopoff  
University of California  
Institute of Geophysics & Planetary Physics  
Los Angeles, CA 90024

Mr. Edward Giller  
Pacific Sierra Research Corp.  
1401 Wilson Boulevard  
Arlington, VA 22209

Prof. L. Timothy Long  
School of Geophysical Sciences  
Georgia Institute of Technology  
Atlanta, GA 30332

Prof. Art McGarr  
Mail Stop 977  
Geological Survey  
345 Middlefield Rd.  
Menlo Park, CA 94025

Dr. George Mellman  
Sierra Geophysics  
11255 Kirkland Way  
Kirkland, WA 98033

Prof. John Nabelek  
College of Oceanography  
Oregon State University  
Corvallis, OR 97331

Prof. Geza Nagy  
University of California, San Diego  
Department of Ames, M.S. B-010  
La Jolla, CA 92093

Prof. Amos Nur  
Department of Geophysics  
Stanford University  
Stanford, CA 94305

Prof. Jack Oliver  
Department of Geology  
Cornell University  
Ithaca, NY 14850

Prof. Robert Phinney  
Geological & Geophysical Sciences  
Princeton University  
Princeton, NJ 08544-0636

Dr. Paul Pomeroy  
Rondout Associates  
P.O. Box 224  
Stone Ridge, NY 12484

Dr. Jay Pulli  
RADIX System, Inc.  
2 Taft Court, Suite 203  
Rockville, MD 20850

Dr. Norton Rimer  
S-CUBED  
A Division of Maxwell Laboratory  
P.O. Box 1620  
La Jolla, CA 92038-1620

Prof. Larry J. Ruff  
Department of Geological Sciences  
1006 C.C. Little Building  
University of Michigan  
Ann Arbor, MI 48109-1063

Dr. Richard Sailor  
TASC Inc.  
55 Walkers Brook Drive  
Reading, MA 01867

Thomas J. Sereno, Jr.  
Science Application Int'l Corp.  
10210 Campus Point Drive  
San Diego, CA 92121

John Sherwin  
Teledyne Geotech  
3401 Shiloh Road  
Garland, TX 75041

Prof. Robert Smith  
Department of Geophysics  
University of Utah  
1400 East 2nd South  
Salt Lake City, UT 84112

Prof. S. W. Smith  
Geophysics Program  
University of Washington  
Seattle, WA 98195

Dr. Stewart Smith  
IRIS Inc.  
1616 North Fort Myer Drive  
Suite 1440  
Arlington, VA 22209

Dr. George Sutton  
Rondout Associates  
P.O. Box 224  
Stone Ridge, NY 12484

Prof. L. Sykes  
Lamont-Doherty Geological Observatory  
of Columbia University  
Palisades, NY 10964

Prof. Pradeep Talwani  
Department of Geological Sciences  
University of South Carolina  
Columbia, SC 29208

Prof. Ta-liang Teng  
Center for Earth Sciences  
University of Southern California  
University Park  
Los Angeles, CA 90089-0741

- Dr. R.B. Tittmann  
Rockwell International Science Center  
1049 Camino Dos Rios  
P.O. Box 1085  
Thousand Oaks, CA 91360

Dr. Gregory van der Vink  
IRIS, Inc.  
1616 North Fort Myer Drive  
Suite 1440  
Arlington, VA 22209

Professor Daniel Walker  
University of Hawaii  
Institute of Geophysics  
Honolulu, HI 96822

William R. Walter  
Seismological Laboratory  
University of Nevada  
Reno, NV 89557

Dr. Gregory Wojcik  
Weidlinger Associates  
4410 El Camino Real  
Suite 110  
Los Altos, CA 94022

Prof. John H. Woodhouse  
Hoffman Laboratory  
Harvard University  
20 Oxford St.  
Cambridge, MA 02138

Dr. Gregory B. Young  
ENSCO, Inc.  
5400 Port Royal Road  
Springfield, VA 22151-2388

GOVERNMENT

Dr. Ralph Alewine III  
DARPA/NMRO  
1400 Wilson Boulevard  
Arlington, VA 22209-2308

Mr. James C. Battis  
GL/LWH  
Hanscom AFB, MA 01731-5000

Dr. Robert Blandford  
DARPA/NMRO  
1400 Wilson Boulevard  
Arlington, VA 22209-2308

Eric Chael  
Division 9241  
Sandia Laboratory  
Albuquerque, NM 87185

Dr. John J. Cipar  
GL/LWH  
Hanscom AFB, MA 01731-5000

Mr. Jeff Duncan  
Office of Congressman Markey  
2133 Rayburn House Bldg.  
Washington, DC 20515

Dr. Jack Evernden  
USGS - Earthquake Studies  
345 Middlefield Road  
Menlo Park, CA 94025

Art Frankel  
USGS  
922 National Center  
Reston, VA 22092

Dr. T. Hanks  
USGS  
Nat'l Earthquake Research Center  
345 Middlefield Road  
Menlo Park, CA 94025

Dr. James Hannon  
Lawrence Livermore Nat'l Laboratory  
P.O. Box 808  
Livermore, CA 94550

Paul Johnson  
ESS-4, Mail Stop J979  
Los Alamos National Laboratory  
Los Alamos, NM 87545

Janet Johnston  
GL/LWH  
Hanscom AFB, MA 01731-5000

Dr. Katharine Kadinsky-Cade  
GL/LWH  
Hanscom AFB, MA 01731-5000

Ms. Ann Kerr  
IGPP, A-025  
Scripps Institute of Oceanography  
University of California, San Diego  
La Jolla, CA 92093

Dr. Max Koontz  
US Dept of Energy/DP 5  
Forrestal Building  
1000 Independence Avenue  
Washington, DC 20585

Dr. W.H.K. Lee  
Office of Earthquakes, Volcanoes,  
& Engineering  
345 Middlefield Road  
Menlo Park, CA 94025

Dr. William Leith  
U.S. Geological Survey  
Mail Stop 928  
Reston, VA 22092

Dr. Richard Lewis  
Director, Earthquake Engineering & Geophysics  
U.S. Army Corps of Engineers  
Box 631  
Vicksburg, MS 39180

James F. Lewkowicz  
GL/LWH  
Hanscom AFB, MA 01731-5000

Mr. Alfred Lieberman  
ACDA/VI-OA'State Department Bldg  
Room 5726  
320 - 21st Street, NW  
Washington, DC 20451

Stephen Mangino  
GL/LWH  
Hanscom AFB, MA 01731-5000

Dr. Frank F. Pilotte  
HQ AFTAC/TT  
Patrick AFB, FL 32925-6001

• Dr. Robert Masse  
• Box 25046, Mail Stop 967  
• Denver Federal Center  
• Denver, CO 80225

Katie Poley  
CIA-OSWR/NED  
Washington, DC 20505

Art McGarr  
U.S. Geological Survey, MS-977  
345 Middlefield Road  
Menlo Park, CA 94025

Mr. Jack Rachlin  
U.S. Geological Survey  
Geology, Rm 3 C136  
Mail Stop 928 National Center  
Reston, VA 22092

Richard Morrow  
ACDA/VI, Room 5741  
320 21st Street N.W  
Washington, DC 20451

Dr. Robert Reinke  
WL/NTESG  
Kirtland AFB, NM 87117-6008

Dr. Keith K. Nakanishi  
Lawrence Livermore National Laboratory  
P.O. Box 808, L-205  
Livermore, CA 94550

Dr. Byron Ristvet  
HQ DNA, Nevada Operations Office  
Attn: NVCG  
P.O. Box 98539  
Las Vegas, NV 89193

Dr. Carl Newton  
Los Alamos National Laboratory  
P.O. Box 1663  
Mail Stop C335, Group ESS-3  
Los Alamos, NM 87545

Dr. George Rothe  
HQ AFTAC/TGR  
Patrick AFB, FL 32925-6001

Dr. Kenneth H. Olsen  
Los Alamos Scientific Laboratory  
P.O. Box 1663  
Mail Stop C335, Group ESS-3  
Los Alamos, NM 87545

Dr. Alan S. Ryall, Jr.  
DARPA/NMRO  
1400 Wilson Boulevard  
Arlington, VA 22209-2308

Howard J. Patton  
Lawrence Livermore National Laboratory  
P.O. Box 808, L-205  
Livermore, CA 94550

Dr. Michael Shore  
Defense Nuclear Agency/SPSS  
6801 Telegraph Road  
Alexandria, VA 22310

• Mr. Chris Paine  
• Office of Senator Kennedy  
• SR 315  
• United States Senate  
• Washington, DC 20510

Donald L. Springer  
Lawrence Livermore National Laboratory  
P.O. Box 808, L-205  
Livermore, CA 94550

Colonel Jerry J. Perrizo  
AFOSR/NP, Building 410  
Bolling AFB  
Washington, DC 20332-6448

Mr. Charles L. Taylor  
GL/LWG  
Hanscom AFB, MA 01731-5000

Dr. Thomas Weaver  
Los Alamos National Laboratory  
P.O. Box 1663, Mail Stop C335  
Los Alamos, NM 87545

DARPA/PM  
1400 Wilson Boulevard  
Arlington, VA 22209

J.J. Zucca  
Lawrence Livermore National Laboratory  
Box 808  
Livermore, CA 94550

Defense Technical Information Center  
Cameron Station  
Alexandria, VA 22314 (5 copies)

GL/SULL  
Research Library  
Hanscom AFB, MA 01731-5000 (2 copies)

Defense Intelligence Agency  
Directorate for Scientific &  
Technical Intelligence/DSTIB  
Washington, DC 20340-6158

Secretary of the Air Force  
(SAFRD)

AFTAC/CA  
(STINFO)  
Patrick AFB, FL 32925-6001

Washington, DC 20330

Office of the Secretary Defense  
DDR & E  
Washington, DC 20330

TACTEC  
Battelle Memorial Institute  
505 King Avenue  
Columbus, OH 43201 (Final Report Only)

HQ DNA  
Attn: Technical Library  
Washington, DC 20305

DARPA/RMO/RETRIEVAL  
1400 Wilson Boulevard  
Arlington, VA 22209

DARPA/RMO/Security Office  
1400 Wilson Boulevard  
Arlington, VA 22209

Geophysics Laboratory  
Attn: XO  
Hanscom AFB, MA 01731-5000

Geophysics Laboratory  
Attn: LW  
Hanscom AFB, MA 01731-5000

CONTRACTORS (Foreign)

Dr. Ramon Cabre, S.J.  
Observatorio San Calixto  
Casilla 5939  
La Paz, Bolivia

Prof. Hans-Peter Harjes  
Institute for Geophysik  
Ruhr University/Bochum  
P.O. Box 102148  
4630 Bochum 1, FRG

Prof. Eystein Husebye  
NTNF/NORSAR  
P.O. Box 51  
N-2007 Kjeller, NORWAY

Prof. Brian L.N. Kennett  
Research School of Earth Sciences  
Institute of Advanced Studies  
G.P.O. Box 4  
Canberra 2601, AUSTRALIA

Dr. Bernard Massinon  
Societe Radiomana  
27 rue Claude Bernard  
75005 Paris, FRANCE (2 Copies)

Dr. Pierre Mecheler  
Societe Radiomana  
27 rue Claude Bernard  
75005 Paris, FRANCE

Dr. Svein Mykkeltveit  
NTNF/NORSAR  
P.O. Box 51  
N-2007 Kjeller, NORWAY

FOREIGN (Others)

Dr. Peter Basham  
Earth Physics Branch  
Geological Survey of Canada  
1 Observatory Crescent  
Ottawa, Ontario, CANADA K1A 0Y3

Dr. Eduard Berg  
Institute of Geophysics  
University of Hawaii  
Honolulu, HI 96822

Dr. Michel Bouchon  
I.R.I.G.M.-B.P. 68  
38402 St. Martin D'Herès  
Cedex, FRANCE

Dr. Hilmar Bungum  
NTNF/NORSAR  
P.O. Box 51  
N-2007 Kjeller, NORWAY

Dr. Michel Campillo  
Observatoire de Grenoble  
I.R.I.G.M.-B.P. 53  
38041 Grenoble, FRANCE

Dr. Kin Yip Chun  
Geophysics Division  
Physics Department  
University of Toronto  
Ontario, CANADA M5S 1A7

Dr. Alan Douglas  
Ministry of Defense  
Blacknest, Brimpton  
Reading RG7-4RS, UNITED KINGDOM

Dr. Roger Hansen  
NTNF/NORSAR  
P.O. Box 51  
N-2007 Kjeller, NORWAY

Dr. Manfred Henger  
Federal Institute for Geosciences & Nat'l Res.  
Postfach 510153  
D-3000 Hanover 51, FRG

Ms. Eva Johannisson  
Senior Research Officer  
National Defense Research Inst.  
P.O. Box 27322  
S-102 54 Stockholm, SWEDEN

Dr. Fekadu Kebede  
Seismological Section  
Box 12019  
S-750 Uppsala, SWEDEN

Dr. Tormod Kvaerna  
NTNF/NORSAR  
P.O. Box 51  
N-2007 Kjeller, NORWAY

Dr. Peter Marshal  
Procurement Executive  
Ministry of Defense  
Blacknest, Brimpton  
Reading FG7-4RS, UNITED KINGDOM

Prof. Ari Ben-Menahem  
Department of Applied Mathematics  
Weizman Institute of Science  
Rehovot, ISRAEL 951729

Dr. Robert North  
Geophysics Division  
Geological Survey of Canada  
1 Observatory Crescent  
Ottawa, Ontario, CANADA K1A 0Y3

Dr. Frode Ringdal  
NTNF/NORSAR  
P.O. Box 51  
N-2007 Kjeller, NORWAY

Dr. Jorg Schlittenhardt  
Federal Institute for Geosciences & Nat'l Res.  
Postfach 510153  
D-3000 Hannover 51, FEDERAL REPUBLIC OF  
GERMANY